The HKU Scholars Hub   The University of Hong Kong   香港大學學術庫

Title	0- transition characteristic of the Josephson current in a carbon nanotube quantum dot
Author(s)	Li, L; Zheng, BB; Chen, W; Chen, H; Luo, HG; Zhang, F
Citation	Physical Review B (Condensed Matter and Materials Physics), 2014, v. 89 n. 24, article no. 245135, p. 245135:1-7
Issued Date	2014
URL	http://hdl.handle.net/10722/203323
Rights	Physical Review B (Condensed Matter and Materials Physics). Copyright © American Physical Society.

0-π transition characteristic of the Josephson current in a carbon nanotube quantum dot

Lin Li,[1,2] Bao-Bing Zheng,[3] Wei-Qiang Chen,[2] Hua Chen,[4] Hong-Gang Luo,[3,5,*] and Fu-Chun Zhang[1,4]

[1]*Department of Physics and Center of Theoretical and Computational Physics, The University of Hong Kong, Hong Kong, China*
[2]*Department of Physics, South University of Science and Technology of China, Shenzhen 518005, China*
[3]*Center of Interdisciplinary Studies and Key Laboratory for Magnetism and Magnetic Materials of the Ministry of Education,*
Lanzhou University, Lanzhou 730000, China
[4]*Department of Physics, Zhejiang University, Hangzhou 310027, China*
[5]*Beijing Computational Science Research Center, Beijing 100084, China*

We consider the Josephson current through the carbon nanotube quantum dot with twofold orbital degeneracy connected by two superconductor leads. We show that the removal of orbital and spin degeneracies due to strong spin-orbit coupling and external magnetic field has a significant influence on the subgap Andreev bound states and the 0-π transition of the Josephson current. The 0-π transition point is determined by the level crossing of the lowest branch of the bound states and the Fermi level, and is given by $[T_K - \Delta_{SO}/2 - (\mu + 1)B]/\Delta \sim 1$, with T_K as the Kondo temperature, Δ_{SO} the spin-orbit coupling, Δ the superconducting gap, μ the ratio of orbital moment and Bohr magneton, and B the Zeeman splitting loaded by the magnetic field. The interplay of the Kondo effect and superconductivity in such a quantum dot device provides a route to manipulate the 0-π transition of the Josephson current.

PACS number(s): 74.50.+r, 72.15.Qm, 73.21.La, 75.20.Hr

I. INTRODUCTION

The study of the Josephson current in a superconductor-nanostructure-superconductor structure has attracted great attention in the past two decades. In particular, when the nanostructure is a quantum dot in the Kondo regime, the Josephson current will be affected by the competition between the Kondo effect characterized by Kondo temperature T_K and the superconductivity characterized by the gap Δ [1–19]. If $T_K \gg \Delta$, the Kondo screening dominates the system, so the ground state of the dot is a Kondo singlet. On the other hand, if $T_K \ll \Delta$, the ground state is a magnetic doublet [2,3] or a BCS-like singlet state [7,9], depending on the parameters such as the dot level ε_d, the Coulomb repulsion U, and the coupling Γ [13–15,20,21]. The Josephson junction is a 0 junction in the former case, and is a π junction due to the reversal of the spin in the Cooper pairs in the latter case [2,3,7,9,10,12,16,19]. Thus a 0-π transition is expected and suggested to occur around $T_K/\Delta \sim 1$ by previous theoretical and experimental studies [3,4,7,9,11]. The transition can be clarified by identifying the Andreev bound states formed by the coherent superposition of all possible Andreev reflection processes [10,21–23].

The Kondo effect in simplest SU(2) quantum dots have been studied intensively and are well understood now. The attention is now focused on the system with more complex structures. In a carbon nanotube, twofold orbital degeneracies arises from the two equivalent valley (K and K') in graphene and corresponds to the clockwise and counterclockwise electron orbits encircling the nanotube [24]. The symmetry group becomes SU(4) when both spin and orbital degree of freedom is considered. The pure orbital Kondo effect [25] and the SU(4) Kondo effect have been investigated in the carbon nanotube quantum dot [26–29]. Some experiments indicate

strong spin-orbit coupling Δ_{SO} in the nanotubes [30–34]. The spin-orbit coupling will break the SU(4) symmetry and hence affect the Kondo transports in the nanotube quantum dot [34–37]. The presence of strong spin-orbit coupling makes the carbon nanotube a good candidate for observing the Majorana bound states [38–40], which is a hot topic in the search of Majorana fermions [38–46]. Here we would like to focus on the effect of the spin-orbit coupling on the Josephson current. In a recent work, Lim, Lopez, and Aguado [47] have studied the Josephson current in a carbon nanotube quantum dot with spin-orbit coupling. They found that the spin-orbit coupling can induce a 0-π transition in the Josephson current in the noninteracting case. They proposed a rich phase diagram in the large gap limit for the Coulomb blockade switched on. Finally, they found that the 0 phase always prevails in the Kondo regime [47,48]. However, the 0-π transition dominated by the competition between Kondo effect and superconductivity in the presence of spin-orbit coupling and Zeeman splitting has not been discussed in this work. This motivates us to further identify the condition under which the 0-π transition happens and to compare our results with the simple SU(2) case.

In the case with SU(2) symmetry, the 0-π transition can be determined by the position of the degenerated subgap bound states in the local density of states (LDOS), as illustrated schematically in Figs. 1(a) and 1(d), where only the particle part of the subgap bound states is depicted for simplicity. These subgap bound states originate from the interplay of the magnetism and superconductivity [49–51] (Yu-Shiba-Rusinov states) and bring about the Andreev bound states in the transport spectrum resorting to the Andreev reflection process. When the position of the bound states cross the Fermi level from below, the Josephson junction changes from π junction to 0 junction, while the ground state of the quantum dot changes from magnetic doublet to Kondo singlet simultaneously. We found that the SU(4) case is similar to the SU(2) one, where the transition occurs around $T_K/\Delta \sim 1$. But the presence of the spin-orbit coupling Δ_{SO} and external magnetic field
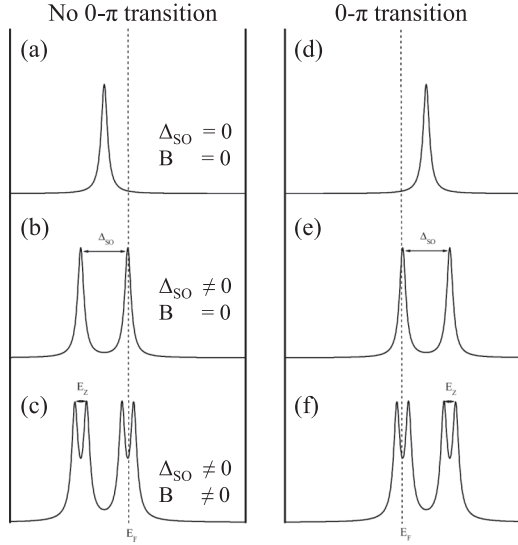
*Corresponding author: luohg@lzu.edu.cn

FIG. 1. Schematic diagram of the dependence of the 0-π transition on the position of the subgap bound states in local density of states (LDOS). Here only the particle channel is presented and that of the hole channel is omitted for simplification. (a)–(c) No 0-π transition if the subgap bound states locate below the Fermi level, even the splitting subgap bound states cross the Fermi level when Δ_{SO} and B are nonzero. (d)–(f) The 0-π transition occurs when the lowest branch of splitting bound states crosses the Fermi level.

significantly change the 0-π transition point. In presence of spin-orbit coupling and Zeeman splitting, the degeneracy of the subgap bound states are lifted [Figs. 1(b), 1(c), 1(e), and 1(f)]. If the ground state of the dot is a magnetic doublet [Figs. 1(b) and 1(c)], there is no 0-π transition even when a bound state crosses the Fermi level. On the other hand, if the ground state of the dot is a Kondo singlet [Figs. 1(e) and 1(f)], the 0-π transition happens when the lowest branch of the bound states cross the Fermi level. It is found that the 0-π transition happens roughly around $(T_K^{SU(4)} - \Delta_{SO}/2)/\Delta \sim 1$ in the presence of spin-orbit coupling and around $[T_K^{SU(4)} - \Delta_{SO}/2 - (\mu + 1)B]/\Delta \sim 1$, when the spin degeneracy is lifted by an additional external magnetic field. In the following, we will present explicit results based on the model calculation.

The paper is organized as follows. In Sec. II we present the model of the superconductor-carbon nanotube quantum dot-superconductor device and its transport formalism. In Sec. III we present explicit results. A brief summary is provided in Sec. IV.

II. MODEL AND FORMALISM

We consider a carbon nanotube quantum dot, which is described by a single impurity Anderson model, connected by two superconductor leads. The Hamiltonian reads

$$H = H_D + H_S + H_T, \quad (1)$$

which describes the dot, the superconducting leads, and the tunneling between them, respectively.

$$H_D = \sum_m \varepsilon_m d_m^\dagger d_m + \frac{U}{2} \sum_{m \neq m'} \hat{n}_m \hat{n}_{m'}, \quad (2)$$

where ε_m is the dot level with $m = \{\lambda, \sigma\}$, the orbital ($\lambda = \pm 1$), and the spin ($\sigma = \pm 1/2$) indices. $d_m^\dagger$ (d_m) is the creation (annihilation) operator of an electron in the dot, and U is the on-site Coulomb repulsion. In the presence of spin-orbit coupling, the dot level becomes

$$\varepsilon_m = \varepsilon_{\lambda\sigma} = \varepsilon_d + \frac{1}{2}\lambda\sigma\Delta_{SO}, \quad (3)$$

ε_d is the bared dot level which can be tuned by the gate voltage, and the second term is the modification due to the spin-orbit coupling. When the magnetic field is applied parallel to the axis of the carbon nanotube, the dot level includes the additional orbital and spin Zeeman splitting, namely,

$$\varepsilon_{\lambda\sigma} = \varepsilon_d + \frac{1}{2}\lambda\sigma\Delta_{SO} + \lambda\mu B + \sigma B, \quad (4)$$

where $B = g\mu_B \mathbf{B}$ is Zeeman energy, $\mu = 2\mu_{orb}/(g\mu_B)$ is the ratio between the orbital magnetic moment μ_{orb} and the Bohr magneton μ_B, and g is the Landé g factor [35]. It was found that μ_{orb} is usually 10–20 times larger than μ_B [30]. The Hamiltonian

$$H_S = \sum_{km\alpha} \varepsilon_{km\alpha} c_{km\alpha}^\dagger c_{km\alpha} - \sum_{km\alpha}(\Delta_\alpha c_{km\alpha}^\dagger c_{\bar{k}\bar{m}\alpha}^\dagger + \text{H.c.}), \quad (5)$$

where $\varepsilon_{km\alpha}$ is the single-particle energy of the electron in the left (right) leads ($\alpha = L, R$), $c_{km\alpha}^\dagger$ ($c_{km\alpha}$) represents the creation (annihilation) operator of electron in the leads, and $\Delta_\alpha = \Delta e^{-i\phi_\alpha}$ is the energy gap with phase ϕ_α. For simplicity we consider that the left and right leads have the same superconducting gap. Finally,

$$H_T = \sum_{km\alpha}(V_{km\alpha} c_{km\alpha}^\dagger d_m + V_{km\alpha}^* d_m^\dagger c_{km\alpha}) \quad (6)$$

describes the hybridization between the dot and the leads, and $V_{km\alpha}$ is the hybridization strength. By using a standard equation of motion approach, which captures the essential physics here, one obtains the dot Green's functions by using the Lacroix's truncation approximation [52]. Consider the large-U limit, the Green's function $G_m(\varepsilon) = \langle\langle d_m; d_m^\dagger \rangle\rangle_\varepsilon$ is given approximately by

$$G_m(\varepsilon) = \frac{1 - \sum_{m' \neq m} \langle \hat{n}_{m'} \rangle - \tilde{A}_m(\varepsilon)}{\varepsilon - \varepsilon_m - \Sigma(\varepsilon)}, \quad (7)$$

where the occupation

$$\langle n_m \rangle = -\frac{1}{\pi} \int \text{Im}[G_m(\varepsilon)] f(\varepsilon) d\varepsilon, \quad (8)$$

$$f(\varepsilon) = \frac{1}{\Gamma(\varepsilon)} \sum_\alpha \Gamma_\alpha(\varepsilon) f_\alpha(\varepsilon), \quad (9)$$

and

$$\Sigma(\varepsilon) = \Sigma_0(\varepsilon)[1 - \tilde{A}_m(\varepsilon)] + \tilde{B}_m(\varepsilon) - \Delta^2 \Pi_m(\varepsilon), \quad (10)$$

$$\Sigma_0(\varepsilon) = -i \sum_\alpha \Gamma_\alpha(\varepsilon), \quad (11)$$

$$\tilde{A}_m(\varepsilon) = \sum_{m' \neq m} A_{m'm}(\varepsilon), \quad (12)$$

$$\tilde{B}_m(\varepsilon) = \sum_{m' \neq m} B_{m'm}(\varepsilon), \tag{13}$$

with $\Gamma_\alpha(\varepsilon) = \Gamma_{0\alpha}\beta(\varepsilon)$, $\Gamma_{0\alpha} = \pi|V_\alpha|^2\rho_0$, $\rho_0 = 1/2D$ is the constant density of states in the normal state, and

$$\beta(\varepsilon) = \frac{\theta(|\varepsilon| - \Delta)|\varepsilon|}{\sqrt{\varepsilon^2 - \Delta^2}} + \frac{\theta(|\varepsilon| - \Delta)\varepsilon}{i\sqrt{\Delta^2 - \varepsilon^2}} \tag{14}$$

is the dimensionless BCS density of states. The other notations introduced are

$$A_{m'm}(\varepsilon) = \frac{1}{\pi} \int \frac{\Gamma(\varepsilon)f(\varepsilon)[\text{Re}G_m(\varepsilon) + \Delta\Xi_{1m}(\varepsilon)]}{\omega - \varepsilon_m + \varepsilon_{m'} - \varepsilon} d\varepsilon, \tag{15}$$

$$B_{m'm}(\varepsilon) = \frac{1}{\pi} \int \frac{\Gamma(\varepsilon)f(\varepsilon) + \tilde{\Gamma}(\varepsilon)\tilde{f}(\varepsilon)(1 - \Delta^2)\text{Im}G_m(\varepsilon)}{\omega - \varepsilon_m + \varepsilon_{m'} - \varepsilon} d\varepsilon, \tag{16}$$

where

$$\tilde{f}(\varepsilon) = \frac{1}{\tilde{\Gamma}(\varepsilon)} \sum_\alpha \Gamma_{\alpha'}(\varepsilon)\Gamma_\alpha(\varepsilon)f_\alpha(\varepsilon)[1 - f_{\alpha'}(\varepsilon)], \tag{17}$$

with $\Gamma(\varepsilon) = \sum_\alpha \Gamma_\alpha(\varepsilon)$, $\tilde{\Gamma}(\varepsilon) = \Gamma_L(\varepsilon)\Gamma_R(\varepsilon)$, and

$$\Xi_{1m}(\varepsilon) = \sum_\alpha [\cos\phi_\alpha \text{Re}F_{m,\bar{m}}(\varepsilon) - \sin\phi_\alpha \text{Im}F_{m,\bar{m}}(\varepsilon)], \tag{18}$$

where $F_{m,\bar{m}}(\varepsilon) = \langle\langle d^\dagger_{\bar{m}}; d^\dagger_m \rangle\rangle_\varepsilon$ is the anomalous dot Green function. $f_\alpha(\varepsilon)$ is the Fermi function of electrons in the leads α. The notation $\Pi_m(\varepsilon)$ reads

$$\Pi_m(\varepsilon) = \sum_{m' \neq m} [C_{m'm}(\varepsilon) + \langle\hat{n}_{m'}\rangle\Sigma_0(\varepsilon)] - D_m(\varepsilon), \tag{19}$$

where

$$C_{m'm}(\varepsilon) = \frac{1}{\pi} \int \frac{\sum_\alpha \Gamma_\alpha(\varepsilon)e^{i\phi_\alpha}f_\alpha(\varepsilon)[\Xi_{2m}(\varepsilon) + \text{Re}F_{m,\bar{m}}(\varepsilon)]}{\omega - \varepsilon_m + \varepsilon_{m'} - \varepsilon} d\varepsilon, \tag{20}$$

$$D_m(\varepsilon) = \frac{(1 - N_m)\Sigma_1(\varepsilon)\Sigma_2(\varepsilon)\left[1 - \sum_{m' \neq m}\langle\hat{n}_{m'}\rangle - \tilde{A}_m(\varepsilon)\right]}{\varepsilon + \varepsilon_{\bar{m}} - (1 - N_m)\Sigma_0(\varepsilon)}, \tag{21}$$

with

$$\Sigma_{1(2)}(\varepsilon) = \sum_\alpha e^{\mp i\phi_\alpha}\frac{\Delta}{\varepsilon}\Gamma_\alpha(\varepsilon) \tag{22}$$

and

$$\Xi_{2m}(\varepsilon) = \sum_\alpha [\cos\phi_\alpha \text{Re}G_m(\varepsilon) + \sin\phi_\alpha \text{Im}G_m(\varepsilon)]. \tag{23}$$

The anomalous Green function we obtained is

$$F_{m,\bar{m}}(\varepsilon) = \frac{(1 - N_m)\Sigma_1(\varepsilon)}{\varepsilon + \varepsilon_{-m} - (1 - N_m)\Sigma_0(\varepsilon)}G_m(\varepsilon), \tag{24}$$

with $N_m = \sum_{m' \neq \bar{m},m}\langle\hat{n}_{m'}\rangle$. With the above formulism, the dot (anomalous) Green functions can be calculated self-consistently.

The Josephson current through the dot can be expressed as

$$I_J(\phi) = \frac{4e}{h}\Gamma_0 \sin(\phi/2) \sum_m \int d\varepsilon f(\varepsilon)\text{Im}[g(\varepsilon)F_{m,\bar{m}}(\varepsilon)], \tag{25}$$

where $\Gamma_0 = \sum_\alpha \Gamma_{0\alpha}$, ϕ is the phase difference of the superconductor leads, and $g(\varepsilon) = i\pi\rho_0\beta(\varepsilon)\frac{\Delta}{\varepsilon}$ is the noninteraction anomalous BCS Green function [10]. Based on the above analysis, we can discuss the 0-π phase transition dominated by the Kondo effect and superconductivity even in the presence of spin-orbit coupling and magnetic fields.

III. RESULT AND DISCUSSION

Focusing on the Andreev transport through the carbon nanotube quantum dot, the Kondo temperature is an important energy scale. For the SU(N) Anderson impurity model, the Kondo temperature obtained by the Lacroix's scheme is given by $T_K^{\text{SU}(N)} \sim D\exp\{\pi\varepsilon_d/[(N-1)\Gamma_0]\}$ [26,35,52], where D is the half bandwidth of the leads. Although this is a crude expression for the Kondo temperature, it is sufficient to capture the nature of the Andreev transport and the 0-π transition of the Josephson current originated from the competition between the Kondo effect and superconductivity.

Before presenting our results, it is necessary to confirm the validity of the equation of motion approach. First of all, it should be pointed out that in the absence of the superconductivity, the method is able to obtain qualitatively the Kondo effect [35,53,54]. When the superconductivity is involved, we consider the SU(2) superconducting Anderson impurity model, in which many known results are available [3,4,7,9,10,14,18,55–57]. In Figs. 2(a) and 2(b) we plot the subgap bound states for different impurity energy levels and the Josephson current as a function of the impurity energy levels for different coupling strength. When the subgap bound states shift from $-\Delta$ to Δ, the 0-π transition of the Josephson current occurs as the subgap bound state goes across the Fermi level, which indicates the ground state of the quantum dot is changed from a magnetic doublet to Kondo singlet states. The transition point with the ratio $T_K^{\text{SU}(2)}/\Delta \sim 1$ is in good agreement with the result obtained in previous works, although the quantitative value of this ratio depends explicitly on the different methods [3,4,7,9]. In order to further confirm the validity of the EOM method, in Fig. 2(c) we show the phase diagram of the Kondo singlet and magnetic doublet ground states and compare it with that obtained by precise NRG method [14] with the same model parameters. The qualitative consistency between these two methods shows that the result obtained by EOM is reliable in whole parameter regimes, namely, the main physics in such a system is dominated by the competition between Kondo effect and superconductivity [3,10,18,55–57]. After the validity of EOM method in the SU(2) case is confirmed, one should believe that this method should work well in the SU(4) case.

In the following we will discuss the Josephson current through the carbon nanotube quantum dot in the presence (or absence) of spin-orbit coupling and Zeeman splitting. The superconducting gap Δ is taken as energy units and the bandwidth $D = 10\Delta$. We assume the magnetic field to be much smaller than the gap ($B \ll \Delta$) and neglects its
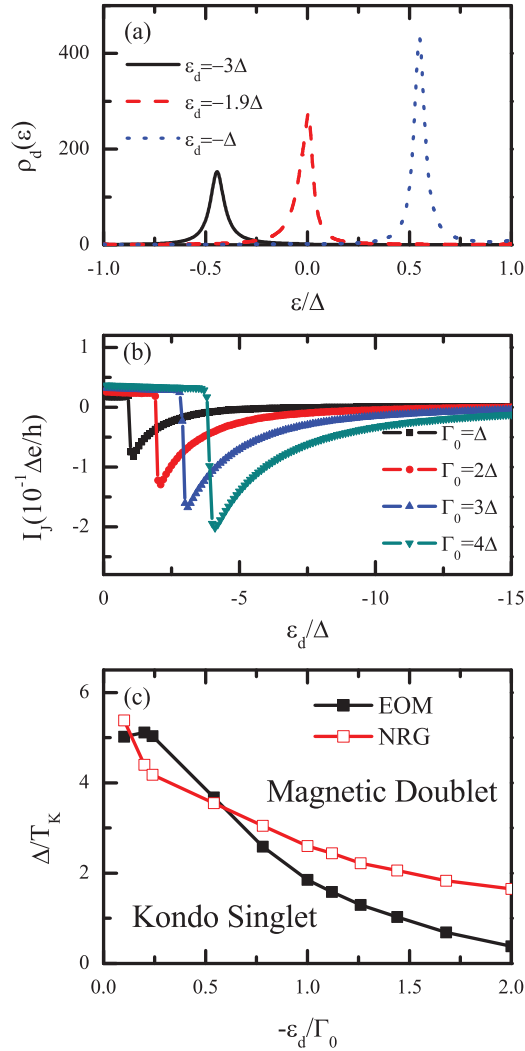
FIG. 2. (Color online) (a) The subgap bound states in LDOS of a SU(2) Anderson impurity attached to superconducting leads with the dot level $\varepsilon_d = (-1, -1.9, -3)\Delta$, the coupling $\Gamma_0(=\Gamma_{0L} + \Gamma_{0R}) = 2\Delta$, the temperature $T = 0$, and the phase difference $\phi = \pi/2$. (b) The 0-π transition of the Josephson current varying with the dot level ε_d and the coupling $\Gamma_0 = (1,2,3,4)\Delta$. (c) The qualitative comparison of the phase diagram of Kondo singlet and magnetic doublet ground states obtain by EOM (black square) and NRG (red empty square) [14] methods in the SU(2) case. The parameters in these two methods are the same.

influence on the superconducting gap for simplification. First of all, we consider the degenerate case, namely, $\Delta_{SO} = B = 0$. Figure 3 shows the Josephson current as a function of the phase difference of the two superconducting leads and the corresponding subgap bound states in the quantum dot. In Figs. 3(a) and 3(c) the subgap bound states is associated with the Andreev bound states which originate from the coherent Andreev reflection processes in which an injecting electron will be reflected as a hole with the time reversal Kramers states [47,58]. In this process, the Kondo resonance plays an important role in enhancement of the Andreev transport [11,12,59,60].

In Fig. 3(a) the tunneling coupling increases gradually, the competition between Kondo correlation and superconductivity
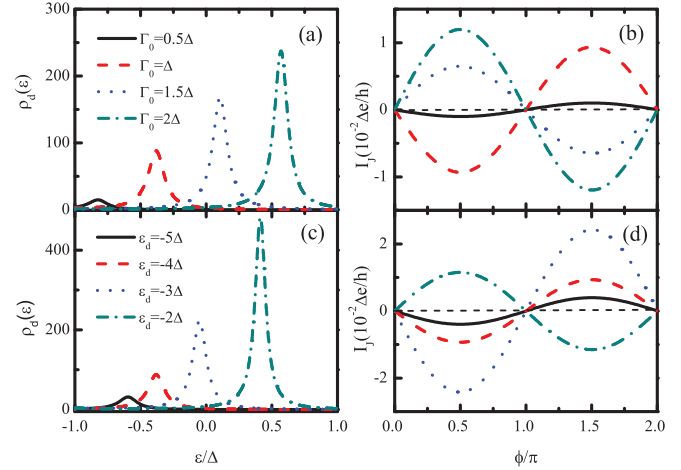

FIG. 3. (Color online) The Kondo temperature (varying with the coupling and level) dependent subgap bound states in LDOS and the current-phase relations. (a) and (b) Different tunneling couplings $\Gamma_0(=\Gamma_{0L} + \Gamma_{0R}) = (0.5, 1, 1.5, 2)\Delta$ with fixed dot level $\varepsilon_d = -4\Delta$. (c) and (d) The dot levels $\varepsilon_d = (-5, -4, -3, -2)\Delta$ with the fixed tunneling coupling $\Gamma_0 = \Delta$. The other parameters used are $\Delta_{SO} = B = 0$, $T = 0$, and $\phi = \pi/2$ in (a) and (c).

is indicated by the position of the subgap bound states. When the Kondo correlation is suppressed by the superconductivity, namely, $T_K^{SU(4)}/\Delta \ll 1$, the subgap bound state is well below the Fermi level and the ground state of the local spin is a magnetic doublet state. In the opposite limit $T_K^{SU(4)}/\Delta \gg 1$, the Kondo screening forms despite the superconductivity and the ground state is a screened singlet state. In this case, the subgap bound state locates above the Fermi level. For $T_K^{SU(4)}/\Delta \sim 1$, the Andreev bound state goes across the Fermi level, which corresponds to the quantum phase transition between the spin singlet and magnetic doublet ground state. As a consequence, the current-phase relation shows a 0-π transition, as shown in Fig. 3(b). The result is in agreement with the picture obtained by the SU(2) Anderson Hamiltonian [3,10]. Similar physics has also been obtained by changing Kondo temperature $T_K^{SU(4)}$ through the dot level, as shown in Figs. 3(c) and 3(d). In Fig. 4 the Josephson current as a function of the dot levels
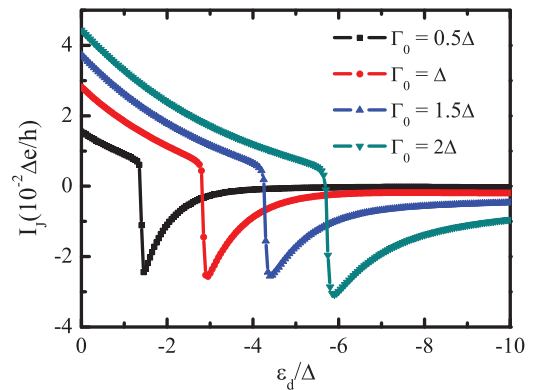

FIG. 4. (Color online) The Josephson current as a function of the dot level for different dot-lead couplings. The 0-π transition occurs at $T_K^{SU(4)}/\Delta \sim 1$. The other parameters used are $\Delta_{SO} = B = 0$ and $\phi = \pi/2$.
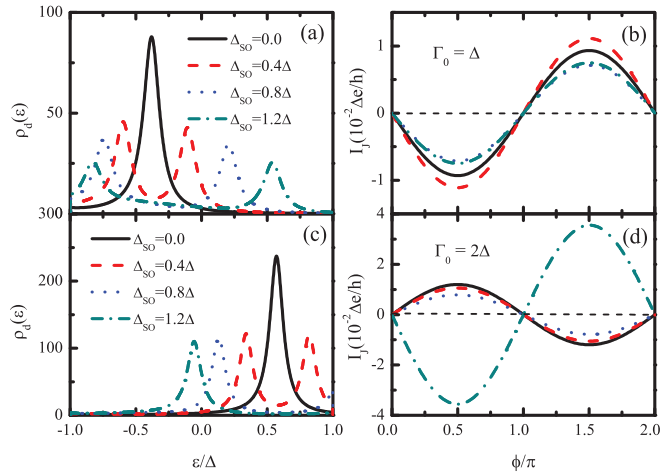
FIG. 5. (Color online) The splitting of subgap bound state in LDOS and the current-phase relations with the spin-orbit coupling $\Delta_{SO} = (0,0.4,0.8,1.2)\Delta$. (a) and (b) $\Gamma_0 = \Delta$ and (c) and (d) $\Gamma_0 = 2\Delta$. The other parameters used are $\varepsilon_d = -4\Delta, B = 0$, and $\phi = \pi/2$ in (a) and (c).

is shown explicitly. For different dot-lead coupling, the 0-π transition point shifts, which is in agreement with $T_K^{SU(4)}/\Delta \sim 1$, as obtained in the previous works [3,4,7,9].

In Fig. 5 we show the case in the presence of spin-orbit coupling, which leads to the splitting of subgap bound states due to the SU(4) symmetry breaking of the quantum dot, as shown in Figs. 5(a) and 5(c). When the degenerate subgap bound state locates below the Fermi level, though the upper branch of the splitting bound states goes across the Fermi level, no 0-π transition happens as shown in Fig. 5(b), since the ground state is a magnetic doublet state even without spin-orbit coupling. On the contrary, if the degenerate subgap bound state locates above the Fermi level, the lower branch of splitting bound states will go across the Fermi level at about $(T_K^{SU(4)} - \Delta_{SO}/2)/\Delta \sim 1$, as shown in Fig. 5(c). As a consequence, a transition from 0 phase to π phase occurs in the Josephson current as shown in Fig. 5(d). Therefore, a 0-π transition could be observed only under conditions of (i) the Andreev bound states locate above the Fermi level (corresponding to a screened singlet ground state) and (ii) the subgap bound states or the lower branch of splitting counterpart move toward and go across the Fermi level. This could be realized experimentally by spin-orbit coupling. In Fig. 6 we show the Josephson current as a function of the spin-orbit coupling. For weak dot-lead coupling $\Gamma_0 = 0.5\Delta, \Delta$, the ground state is a magnetic doublet state and the quantum dot always shows π junction behavior. While for the coupling $\Gamma_0 = 1.5\Delta, 2\Delta$, the ground state is a screened singlet state and the 0-π transition occurs at $(T_K^{SU(4)} - \Delta_{SO}/2)/\Delta \sim 1$, which means the spin-orbit coupling can lead to 0-π transition by suppression of the Kondo effect.

Furthermore, if the magnetic field is applied, the subgap bound states would further split due to the orbital and spin Zeeman energies, as shown in the inset of Fig. 7. In the absence of the spin-orbit coupling, increasing the magnetic field, a 0-π transition happens at $B = 0.0085\Delta$ roughly $[T_K^{SU(4)} - (\mu + 1)B]/\Delta \sim 1$ as shown in Fig. 7. Considering finite spin-
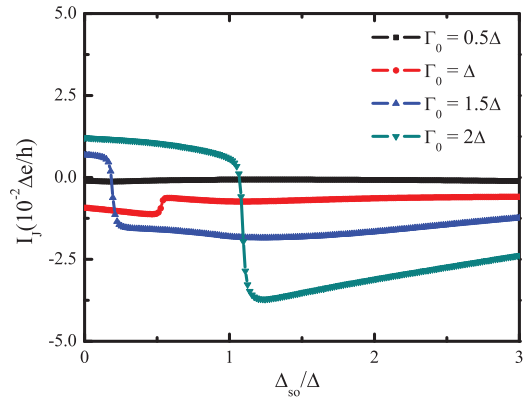

FIG. 6. (Color online) The Josephson current as a function of the spin-orbit coupling. The 0-π transition occurs at $(T_K^{SU(4)} - \Delta_{SO}/2)/\Delta \sim 1$. The other parameters used are $\varepsilon_d = -4\Delta, B = 0$, and $\phi = \pi/2$.

orbit coupling together with the magnetic field, the subgap bound states become four substates due to the degeneracy removed completely, in which two lower substates will move below the Fermi level while increasing the magnetic field. Therefore, one cannot only observe the 0-π transition taking place when the lowest brand of the subgap bound state crosses the Fermi level, the Josephson current shows two dramatic drops, which correspond to other substates going across the Fermi level successively. Roughly, it is found that the 0-π transition occurs around $[T_K^{SU(4)} - \Delta_{SO}/2 - (\mu + 1)B]/\Delta \sim 1$. It indicates the spin-orbit coupling and the Zeeman splitting can independently lead to 0-π transition by suppressing the Kondo effect.

Our results indicate that the spin-orbit coupling and the magnetic field applied have a significant influence on the behavior of the Josephson current in the carbon nanotube quantum dot connected by two superconducting leads. Our results could be observed in a carbon nanotube quantum dot
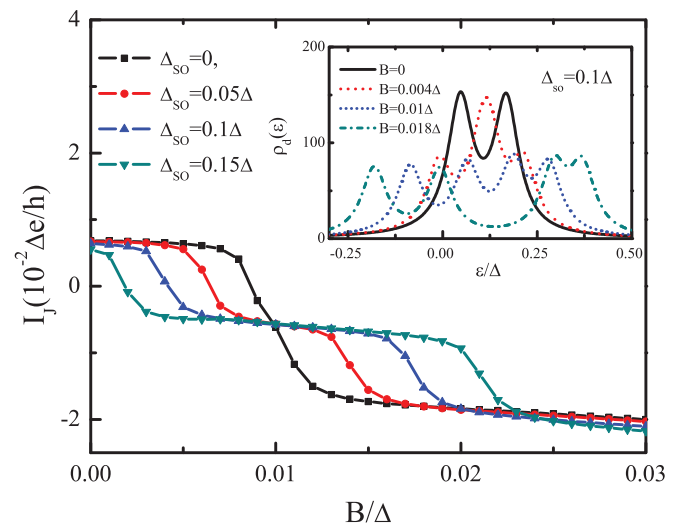

FIG. 7. (Color online) The Josephson current as a function of the magnetic field applied with different spin-orbit couplings. The inset shows the splitting of subgap bound states with different magnetic fields for $\Delta_{SO} = 0.1\Delta$. The other parameters used are $\Gamma_0 = 1.5\Delta, \varepsilon_d = -4\Delta, \phi = \pi/2$, and $\mu = 10$.

strongly coupled with superconducting leads, since the strong spin-orbit coupling induced by curvature has been observed in several kinds of carbon carbon nanotubes [30,31,33,34] and spin-orbit coupling itself can be tuned by the gate voltage [32]. Therefore, our work is useful to stimulate further experiment along this direction.

IV. SUMMARY

In summary, we have studied the 0-π transition in the Josephson current through a strongly correlated carbon nanotube quantum dot with spin-orbit coupling and magnetic field. The competition between the Kondo effect and superconductivity determines the ground state of the carbon nanotube quantum dot, which further determines the property of the subgap bound states and the Josephson current. The presence of the spin-orbit coupling and the magnetic field applied affect dramatically the Josephson current and possible 0-π transition. It is found that it is crucially important for the degenerated subgap bound state to locate above or below the Fermi level determined by the dot parameters, which can be tuned by external electronic fields. The basic picture is schematically summarized in Fig. 1. If the subgap bound state locates below the Fermi level, the ground state of the system is a magnetic doublet and no 0-π transition of the Josephsom current occurs in the presence of spin-orbit coupling and Zeeman splitting. Otherwise, if the degenerated subgap bound state locates above the Fermi level, the ground state is a screened singlet state and the 0-π transition occurs around $[T_K^{\mathrm{SU(4)}} - \Delta_{\mathrm{SO}}/2 - (\mu + 1)B]/\Delta \sim 1$. The presence of spin-orbit coupling and the magnetic field applied provide rich possibility to control the Josephson current, which should be useful in realistic experimental devices.

[1] L. I. Glazman and K. A. Matveev, Pis'ma Zh. Eksp. Teor. Fiz. **49**, 570 (1989) [JETP Lett. **49**, 659 (1989)].

[2] A. V. Rozhkov and D. P. Arovas, Phys. Rev. Lett. **82**, 2788 (1999).

[3] A. A. Clerk and V. Ambegaokar, Phys. Rev. B **61**, 9109 (2000).

[4] A. V. Rozhkov and D. P. Arovas, Phys. Rev. B **62**, 6687 (2000).

[5] M. R. Buitelaar, T. Nussbaumer, and C. Schönenberger, Phys. Rev. Lett. **89**, 256801 (2002).

[6] M. R. Buitelaar, W. Belzig, T. Nussbaumer, B. Babic, C. Bruder, and C. Schönenberger, Phys. Rev. Lett. **91**, 057005 (2003).

[7] M.-S. Choi, M. Lee, K. Kang, and W. Belzig, Phys. Rev. B **70**, 020502(R) (2004).

[8] M. Lee, T. Jonckheere, and T. Martin, Phys. Rev. Lett. **101**, 146804 (2008).

[9] F. Siano and R. Egger, Phys. Rev. Lett. **93**, 047002 (2004).

[10] G. Sellier, T. Kopp, J. Kroha, and Y. S. Barash, Phys. Rev. B **72**, 174502 (2005).

[11] J.-P. Cleuziou, W. Wernsdorfer, V. Bouchiat, T. Ondarcuhu, and M. Monthioux, Nat. Nanotechnol. **1**, 53 (2006).

[12] C. Buizert, A. Oiwa, K. Shibata, K. Hirakawa, and S. Tarucha, Phys. Rev. Lett. **99**, 136806 (2007).

[13] Y. Tanaka, A. Oguri, and A. C. Hewson, New J. Phys. **9**, 115 (2007).

[14] J. S. Lim and M.-S. Choi, J. Phys.: Condens. Matter **20**, 415225 (2008).

[15] C. Karrasch, A. Oguri, and V. Meden, Phys. Rev. B **77**, 024517 (2008).

[16] C. Karrasch and V. Meden, Phys. Rev. B **79**, 045110 (2009).

[17] R. Žitko, M. Lee, R. López, R. Aguado, and M.-S. Choi, Phys. Rev. Lett. **105**, 116803 (2010).

[18] A. Martín-Rodero and A. Levy Yeyati, Adv. Phys. **60**, 899 (2011).

[19] D. J. Luitz, F. F. Assaad, T. Novotny, C. Karrasch, and V. Meden, Phys. Rev. Lett. **108**, 227001 (2012).

[20] J. Bauer, A. Oguri, and A. C. Hewson, J. Phys.: Condens. Matter **19**, 486211 (2007).

[21] T. Meng, S. Florens, and P. Simon, Phys. Rev. B **79**, 224521 (2009).

[22] T. Hecht, A. Weichselbaum, J. von Delft, and R. Bulla, J. Phys.: Condens. Matter **20**, 275213 (2008).

[23] R. S. Deacon, Y. Tanaka, A. Oiwa, R. Sakano, K. Yoshida, K. Shibata, K. Hirakawa, and S. Tarucha, Phys. Rev. Lett. **104**, 076805 (2010); Phys. Rev. B **81**, 121308 (2010).

[24] E. D. Minot, Y. Yaish, V. Sazonova, and P. L. McEuen, Nature (London) **428**, 536 (2004).

[25] P. Jarillo-Herrero, J. Kong, H. van der Zant, C. Dekker, L. P. Kouwenhoven, and S. De Franceschi, Nature (London) **434**, 484 (2005).

[26] M.-S. Choi, R. López, and R. Aguado, Phys. Rev. Lett. **95**, 067204 (2005).

[27] J. S. Lim, M.-S. Choi, M. Y. Choi, R. López, and R. Aguado, Phys. Rev. B **74**, 205119 (2006).

[28] A. Makarovski, A. Zhukov, J. Liu, and G. Finkelstein, Phys. Rev. B **75**, 241407(R) (2007).

[29] G. C. Tettamanzi, J. Verduijn, G. P. Lansbergen, M. Blaauboer, M. J. Calderón, R. Aguado, and S. Rogge, Phys. Rev. Lett. **108**, 046803 (2012).

[30] F. Kuemmeth, S. llani, D. C. Ralph, and P. L. McEuen, Nature (London) **452**, 448 (2008).

[31] S. H. Jhang, M. Marganska, Y. Skourski, D. Preusche, B. Witkamp, M. Grifoni, H. van der Zant, J. Wosnitza, and C. Strunk, Phys. Rev. B **82**, 041404(R) (2010).

[32] T. S. Jespersen, K. Grove-Rasmussen, J. Paaske, K. Muraki, T. Fujisawa, J. Nygard, and K. Flensberg, Nat. Phys. **7**, 348 (2011).

[33] G. A. Steele, F. Pei, E. A. Laird, J. M. Jol, H. B. Meerwaldt, and L. P. Kouwenhoven, Nat. Commun. **4**, 1573 (2013).

[34] J.P. Cleuziou, N.V. N'Guyen, S. Florens, and W. Wernsdorfer, Phys. Rev. Lett. **111**, 136803 (2013).

[35] T.-F. Fang, W. Zuo, and H.-G. Luo, Phys. Rev. Lett. **101**, 246805 (2008); **104**, 169902(E) (2010).

[36] M. R. Galpin, F. W. Jayatilaka, D. E. Logan, and F. B. Anders, Phys. Rev. B **81**, 075437 (2010).

[37] D. R. Schmid, S. Smirnov, M. Marganska, A. Dirnaichner, P. L. Stiller, M. Grifoni, A. K. Hüttel, and C. Strunk, arXiv:1312.6586.

[38] J. Klinovaja, S. Gangadharaiah, and D. Loss, Phys. Rev. Lett. **108**, 196804 (2012).

[39] R. Egger and K. Flensberg, Phys. Rev. B **85**, 235462 (2012).

[40] J. D. Sau and S. Tewari, Phys. Rev. B **88**, 054503 (2013).

[41] V. Mourik, K. Zuo, S. M. Frolov, S. R. Plissard, E. P. A. M. Bakkers, and L. P. Kouwenhoven, Science **336**, 1003 (2012).

[42] Y. Oreg, G. Refael, and F. von Oppen, Phys. Rev. Lett. **105**, 177002 (2010).

[43] A. Das, Y. Ronen, Y. Most, Y. Oreg, M. Heiblum, and H. Shtrikman, Nat. Phys. **8**, 887 (2012).

[44] M. T. Deng, C. L. Yu, G. Y. Huang, M. Larsson, P. Caroff, and H. Q. Xu, Nano Lett. **12**, 6414 (2012).

[45] A. D. K. Finck, D. J. Van Harlingen, P. K. Mohseni, K. Jung, and X. Li, Phys. Rev. Lett. **110**, 126406 (2013).

[46] H. O. H. Churchill, V. Fatemi, K. Grove-Rasmussen, M. T. Deng, P. Caroff, H. Q. Xu, and C. M. Marcus, Phys. Rev. B **87**, 241401(R) (2013).

[47] J. S. Lim, R. López, and R. Aguado, Phys. Rev. Lett. **107**, 196801 (2011).

[48] A. Zazunov, A. L. Yeyati, and R. Egger, Phys. Rev. B **81**, 012502 (2010).

[49] L. Yu, Acta Phys. Sin. **21**, 75 (1965).

[50] H. Shiba, Prog. Theor. Phys. **40**, 435 (1968).

[51] A. I. Rusinov, Zh. Eksp. Teor. Fiz. **56**, 2047 (1969) [Sov. Phys. JETP **29**, 1101 (1969)].

[52] C. Lacroix, J. Phys. F **11**, 2389 (1981).

[53] H.-G. Luo, Z.-J. Ying, and S.-J. Wang, Phys. Rev. B **59**, 9710 (1999).

[54] L. Li, Y.-Y. Ni, T.-F. Fang, and H.-G. Luo, Phys. Rev. B **84**, 235405 (2011).

[55] K. J. Franke, G. Schulze, and J. I. Pascual, Science **332**, 940 (2011).

[56] B.-K. Kim, Y.-H. Ahn, J.-J. Kim, M.-S. Choi, M.-H. Bae, K. Kang, J. S. Lim, R. López, and N. Kim, Phys. Rev. Lett. **110**, 076803 (2013).

[57] W. Chang, V. E. Manucharyan, T. S. Jespersen, J. Nygard, and C. M. Marcus, Phys. Rev. Lett. **110**, 217005 (2013).

[58] V. Koerting, B. M. Andersen, K. Flensberg, and J. Paaske, Phys. Rev. B **82**, 245108 (2010).

[59] K. G. Rasmussen, H. I. Jørgensen, and P. E. Lindelof, New J. Phys. **9**, 124 (2007).

[60] A. Eichler, R. Deblock, M. Weiss, C. Karrasch, V. Meden, C. Schönenberger, and H. Bouchiat, Phys. Rev. B **79**, 161407 (2009); A. Eichler, M. Weiss, S. Oberholzer, C. Schönenberger, A. Levy Yeyati, J. C. Cuevas, and A. Martín-Rodero, Phys. Rev. Lett. **99**, 126602 (2007).